Electronic Supporting Information Materials

Synthesis and antitumor mechanisms of two novel platinum(II) complexes with 3-(2′-benzimidazolyl)-7-methoxycoumarin

Qi-Pin Qin [a,c,1], Shu-Long Wang [a,1], Ming-Xiong Tan [a,*], Zhen-Feng Wang [a], Xiao-Ling Huang [a], Qing-Min Wei [a,*], Bei-Bei Shi [a], Bi-Qun Zou [b,c,*] and Hong Liang [c,*]

Table S1. Crystal data and structure refinement details for H-MeOBC.

Empirical formula	$C_{17}N_2O_3$
Formula weight	280.19
Temperature/K	296.15
Crystal system	monoclinic
Space group	$P2_1/c$
a/Å	13.2523(7)
b/Å	8.0408(4)
c/Å	12.7339(6)
α/°	90.00
β/°	91.040(4)
γ/°	90.00
Volume/Å^3	1356.70(11)
Z	4
ρ_{calc}g/cm^3	1.372
μ/mm^{-1}	0.098
F(000)	560.0
Crystal size/mm^3	0.2 × 0.15 × 0.1
Radiation	MoKα (λ = 0.71073)
2Θ range for data collection/°	6.7 to 50
Index ranges	$-12 \le h \le 15$, $-9 \le k \le 9$, $-15 \le l \le 15$
Reflections collected	8840
Independent reflections	2390 [R_{int} = 0.0192, R_{sigma} = 0.0194]
Data/restraints/parameters	2390/0/199
Goodness-of-fit on F^2	1.033
Final R indexes [I>=2σ (I)]	R_1 = 0.0779, wR_2 = 0.2578
Final R indexes [all data]	R_1 = 0.0884, wR_2 = 0.2677
Largest diff. peak/hole / e Å^{-3}	0.75/-0.21

[a] $R_1 = \Sigma\, ||F_o| - |F_c||/\Sigma|F_o|$; [b] $wR_2 = [\Sigma w(F_o^2 - F_c^2)^2/\Sigma w(F_o^2)^2]^{1/2}$.

Table S2. Selected bond lengths (Å) for H-MeOBC.

Atom	Atom	Length/Å	Atom	Atom	Length/Å
O1	C6	1.377(4)	O8	C12	1.215(4)
O1	C12	1.369(4)	C10	C15	1.415(5)
C2	C3	1.358(4)	N11	C13	1.371(4)
C2	C9	1.422(5)	N11	C16	1.379(4)
C3	C12	1.464(4)	C13	N14	1.316(4)
C3	C13	1.456(4)	N14	C17	1.389(4)
C4	C6	1.380(4)	C16	C17	1.395(5)
C4	C10	1.382(5)	C16	C20	1.394(5)
O5	C10	1.359(4)	C17	C21	1.399(5)
O5	C18	1.438(4)	C19	C20	1.387(5)
C6	C9	1.402(4)	C19	C22	1.397(6)
C7	C9	1.417(5)	C21	C22	1.387(5)
C7	C15	1.360(5)			

Table S3. Selected bond angles (°) for H-MeOBC.

Atom	Atom	Atom	Angle/°	Atom	Atom	Atom	Angle/°
C12	O1	C6	123.2(2)	O1	C12	C3	117.6(3)
C3	C2	C9	121.6(3)	O8	C12	O1	116.1(3)
C2	C3	C12	119.4(3)	O8	C12	C3	126.3(3)
C2	C3	C13	121.2(3)	N11	C13	C3	123.6(3)
C13	C3	C12	119.5(3)	N14	C13	C3	123.9(3)
C6	C4	C10	117.6(3)	N14	C13	N11	112.5(3)
C10	O5	C18	117.5(3)	C13	N14	C17	104.9(3)
O1	C6	C4	116.8(3)	C7	C15	C10	119.9(3)
O1	C6	C9	119.6(3)	N11	C16	C17	104.9(3)
C4	C6	C9	123.6(3)	N11	C16	C20	132.4(3)
C15	C7	C9	121.0(3)	C20	C16	C17	122.6(3)
C6	C9	C2	118.6(3)	N14	C17	C16	110.4(3)
C6	C9	C7	116.8(3)	N14	C17	C21	129.6(3)
C7	C9	C2	124.5(3)	C16	C17	C21	120.0(3)
C4	C10	C15	121.1(3)	C20	C19	C22	121.2(3)
O5	C10	C4	124.6(3)	C19	C20	C16	116.8(3)
O5	C10	C15	114.3(3)	C22	C21	C17	117.7(3)
C13	N11	C16	107.2(3)	C21	C22	C19	121.7(3)

Table S4. Crystal data and structure refinement details for **Pt2**.

Empirical formula	$C_{21}H_{23}Cl_3N_2O_5Pt_2S_2$
Formula weight	944.07
Temperature/K	296.15
Crystal system	triclinic
Space group	P-1
a/Å	9.4211(4)
b/Å	12.9359(8)
c/Å	13.8521(8)
α/°	66.332(6)
β/°	88.609(4)
γ/°	71.401(5)
Volume/Å^3	1454.91(16)
Z	2
ρ_{calc}g/cm^3	2.1549
μ/mm^{-1}	10.054
F(000)	879.6
Crystal size/mm^3	0.22 × 0.2 × 0.18
Radiation	Mo Kα (λ = 0.71073)
2Θ range for data collection/°	6.54 to 52.74
Index ranges	$-12 \leq h \leq 12$, $-13 \leq k \leq 17$, $-17 \leq l \leq 18$
Reflections collected	10849
Independent reflections	5931 [R_{int} = 0.0401, R_{sigma} = 0.0827]
Data/restraints/parameters	5931/0/320
Goodness-of-fit on F^2	1.044
Final R indexes [I>=2σ (I)]	R_1 = 0.0528, wR_2 = 0.1259
Final R indexes [all data]	R_1 = 0.0850, wR_2 = 0.1491
Largest diff. peak/hole / e Å^{-3}	4.62/-2.63

[a] $R_1 = \Sigma\, ||F_o| - |F_c||/\Sigma|F_o|$; [b] $wR_2 = [\Sigma w(F_o^2 - F_c^2)^2/\Sigma w(F_o^2)^2]^{½}$.

Table S5. Selected bond lengths (Å) for **Pt2**.

Atom	Atom	Length/Å	Atom	Atom	Length/Å
Pt2	Cl3	2.308(3)	C13	C12	1.375(15)
Pt2	N2	2.049(10)	C10	C11	1.390(16)
Pt2	O3	2.012(10)	C10	C9	1.396(16)
Pt2	S2	2.219(3)	C11	C6	1.378(17)
Pt1	S1	2.209(4)	C12	C9	1.404(15)
Pt1	Cl2	2.311(4)	C16	C21	1.395(17)
Pt1	N1	2.034(10)	C16	C17	1.383(16)
Pt1	Cl1	2.295(4)	C9	C8	1.409(16)
S1	O1	1.431(10)	S2	O2	1.480(10)
S1	C1	1.756(15)	S2	C3	1.775(13)
S1	C2	1.749(15)	S2	C4	1.777(16)
N2	C15	1.371(13)	C20	C19	1.380(19)
N2	C21	1.397(15)	C20	C21	1.388(17)
O3	C14	1.294(14)	C19	C18	1.38(2)
O4	C10	1.393(14)	C17	C18	1.389(19)
O4	C14	1.332(13)	O5	C6	1.352(15)
N1	C15	1.361(14)	O5	C5	1.434(16)
N1	C16	1.394(15)	C6	C7	1.397(17)
C15	C13	1.440(14)	C8	C7	1.348(17)
C13	C14	1.427(15)			

Table S6. Selected bond angles (°) for **Pt2**.

Atom	Atom	Atom	Angle/°	Atom	Atom	Atom	Angle/°
N2	Pt2	Cl3	97.0(3)	C9	C10	O4	119.1(10)
O3	Pt2	Cl3	172.8(3)	C9	C10	C11	124.4(11)
O3	Pt2	N2	89.3(4)	O4	C14	O3	113.4(10)
S2	Pt2	Cl3	87.27(13)	C13	C14	O3	125.0(11)
S2	Pt2	N2	175.7(3)	C13	C14	O4	121.5(10)
S2	Pt2	O3	86.5(3)	C6	C11	C10	117.4(12)
Cl2	Pt1	S1	179.26(15)	C9	C12	C13	122.3(10)
N1	Pt1	S1	90.6(3)	C21	C16	N1	107.9(10)
N1	Pt1	Cl2	88.7(3)	C17	C16	N1	128.5(12)
Cl1	Pt1	S1	91.08(16)	C17	C16	C21	123.5(12)
Cl1	Pt1	Cl2	89.64(18)	C12	C9	C10	118.6(11)
Cl1	Pt1	N1	178.0(3)	C8	C9	C10	114.9(11)
O1	S1	Pt1	116.5(4)	C8	C9	C12	126.5(11)
C1	S1	Pt1	110.9(6)	O2	S2	Pt2	113.2(4)
C1	S1	O1	109.2(8)	C3	S2	Pt2	110.9(6)
C2	S1	Pt1	110.1(6)	C3	S2	O2	108.9(7)
C2	S1	O1	107.4(7)	C4	S2	Pt2	112.1(5)
C2	S1	C1	101.7(9)	C4	S2	O2	108.6(7)
C15	N2	Pt2	122.9(7)	C4	S2	C3	102.5(8)
C21	N2	Pt2	131.3(8)	C21	C20	C19	118.4(14)
C21	N2	C15	105.7(10)	C18	C19	C20	122.2(13)
C14	O3	Pt2	126.6(8)	C16	C21	N2	108.2(11)
C14	O4	C10	121.5(9)	C20	C21	N2	133.3(12)
C15	N1	Pt1	128.6(8)	C20	C21	C16	118.4(12)
C16	N1	Pt1	121.1(8)	C18	C17	C16	116.6(13)
C16	N1	C15	106.3(10)	C17	C18	C19	120.7(13)
N1	C15	N2	111.8(10)	C5	O5	C6	116.7(11)
C13	C15	N2	126.6(10)	O5	C6	C11	124.6(12)
C13	C15	N1	121.6(10)	C7	C6	C11	120.2(12)
C14	C13	C15	121.5(10)	C7	C6	O5	115.1(11)
C12	C13	C15	121.9(10)	C7	C8	C9	122.4(12)
C12	C13	C14	116.6(10)	C8	C7	C6	120.6(12)
C11	C10	O4	116.5(11)				

Table S7. Inhibitory rates (%) of *cis*-$Pt(DMSO)_2Cl_2$, cisplatin, the ligand H-MeOBC, the Pt(II) complexes **Pt1** and **Pt2** toward on the selected six human cells for 48 h.

Compounds	HeLa	Hep-G2	SK-OV-3/DDP	SK-OV-3	MGC80-3	HL-7702
H-OMe	25.06±1.06	28.12±1.74	30.15±2.06	24.18±1.91	20.11±0.75	20.32±0.33
Pt1	38.96±0.51	32.71±1.17	65.13±0.45	35.26±0.52	36.02±1.60	24.03±0.88
Pt2	42.35±1.06	40.15±1.02	85.99±0.29	41.82±1.10	40.56±0.79	23.99±1.78
vehicle (1% DMSO)	10.23±0.56	13.05±2.01	9.15±1.54	13.02±1.97	10.23±1.01	11.04±1.07
cis-$Pt(DMSO)_2Cl_2$ [b]	22.03±1.36	18.06±1.12	23.20±1.05	19.23±0.95	23.54±1.78	25.03±1.65
Cisplatin [b]	62.03±1.13	65.18±0.85	40.15±1.89	59.15±0.52	58.66±0.85	60.23±0.59

Results represent mean ± SD of at least five independent experiments. SD represents the standard deviation. [a] The concentration is 20 μM. [b] The concentration is 100 μM. [c] Cisplatin was dissolved at a concentration of 1.0 mM in 0.154 M NaCl.

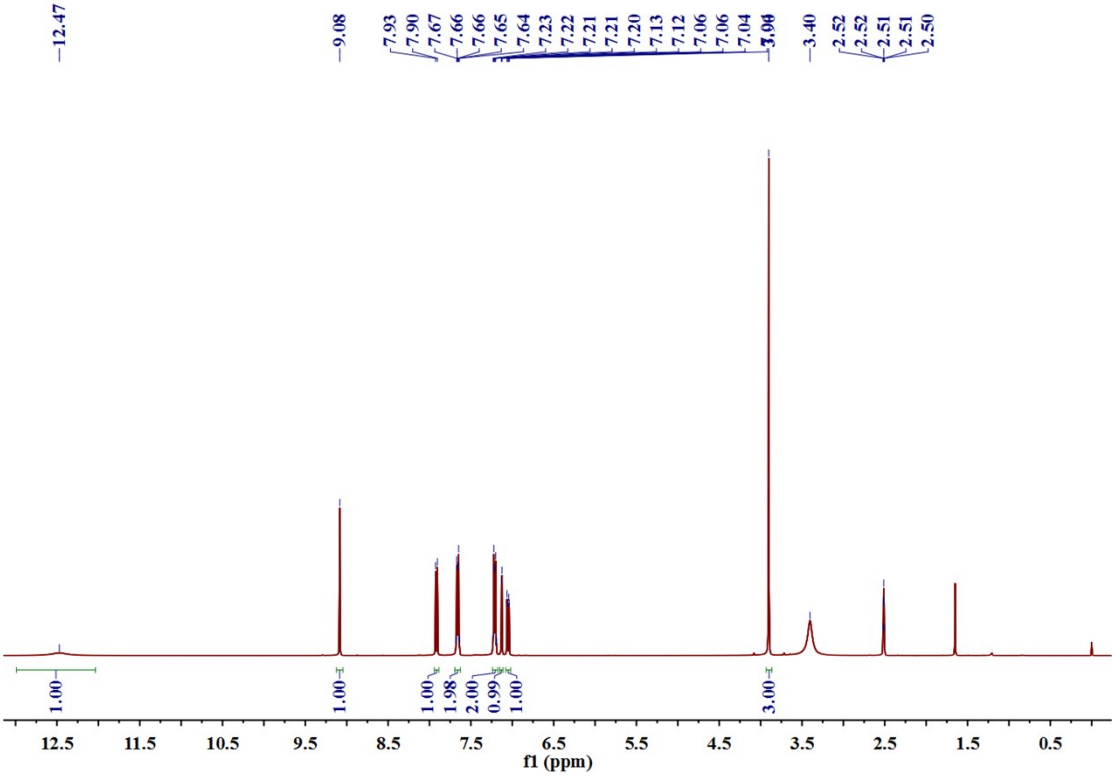

Fig. S1. ^{1}H NMR (400MHz, DMSO-d_6) for the ligand H-MeOBC

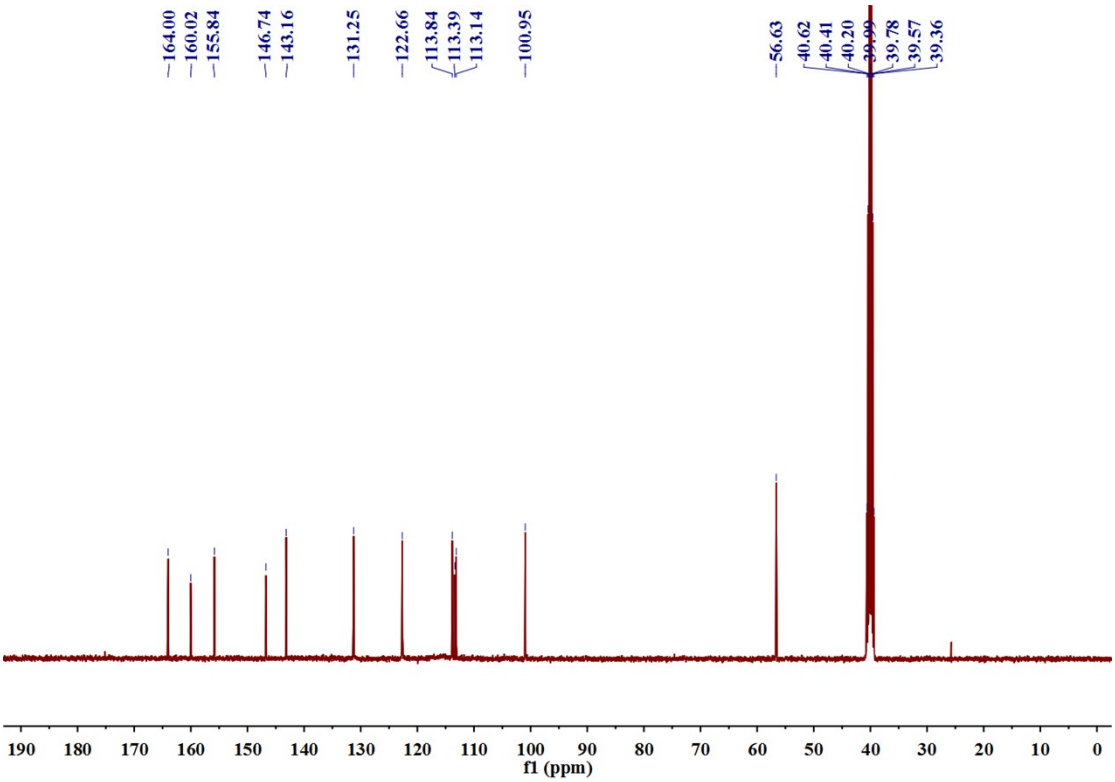

Fig. S2. ^{13}C NMR (101MHz, DMSO-d_6) for the ligand H-MeOBC

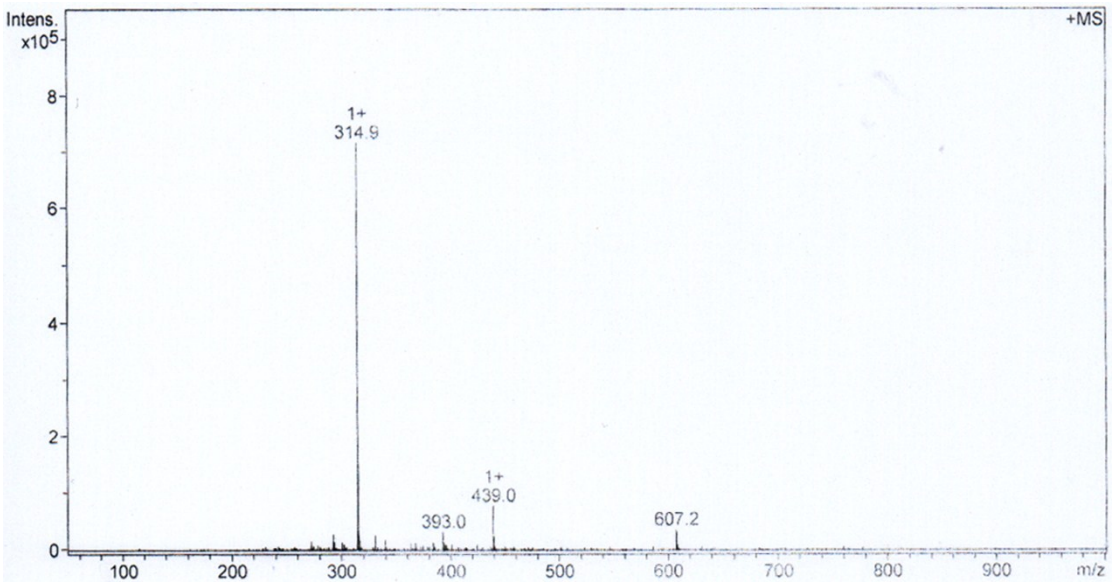

Fig. S3. ESI-MS spectra of the ligand H-MeOBC

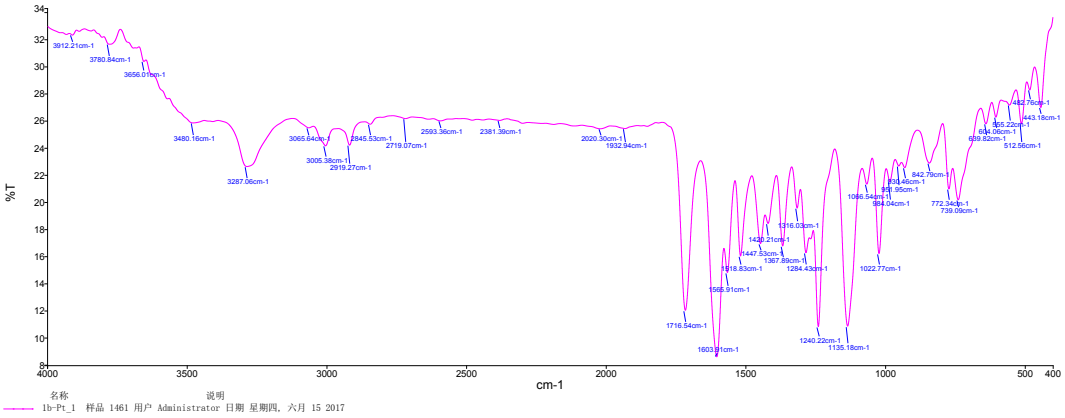

Fig. S4. IR (KBr) spectra of **Pt1**

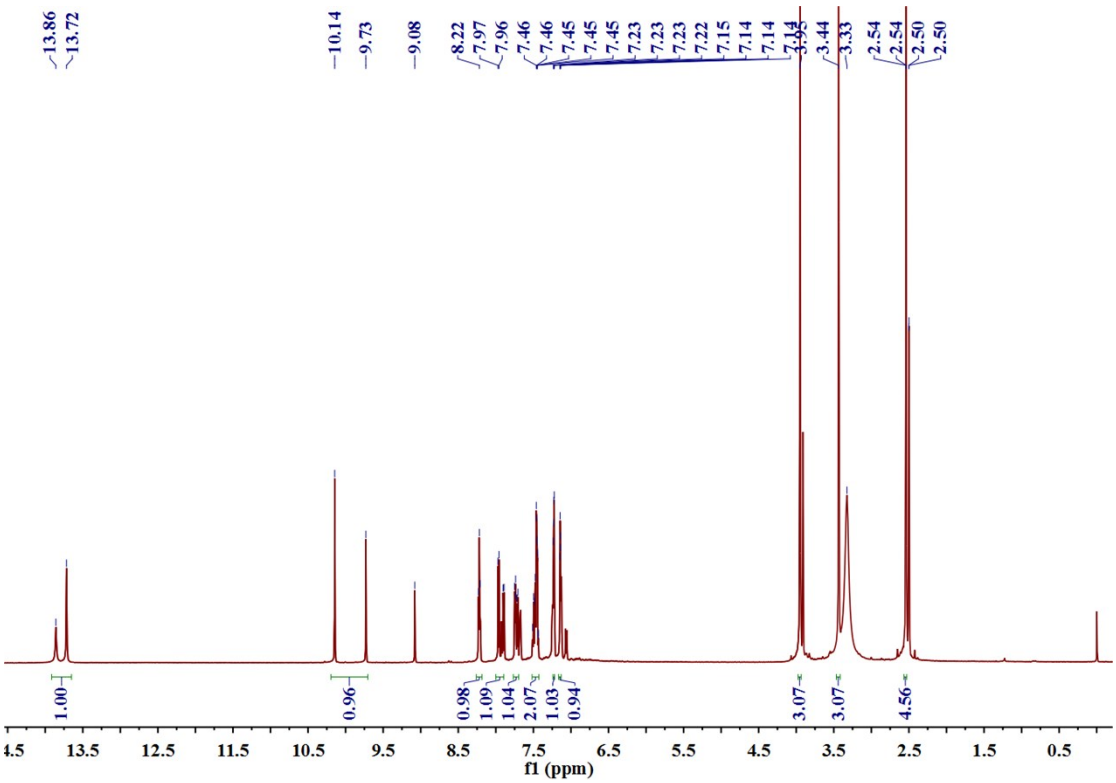

Fig. S5. ^{1}H NMR (600MHz, DMSO-d_6) for **Pt1**

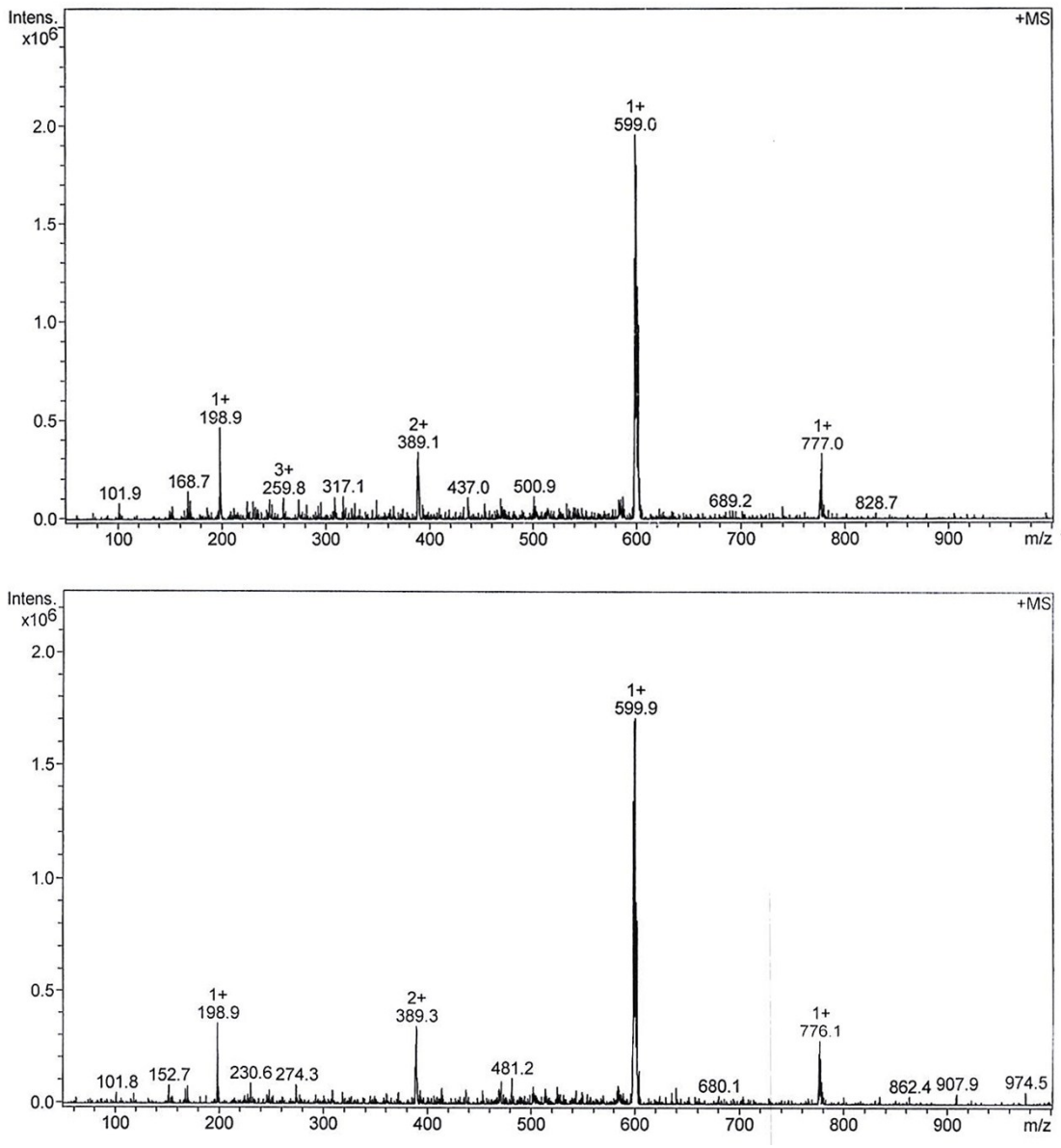

Fig. S6. The mass spectra of **Pt1** in Tris-HCl buffer solution (containing 5% DMSO) for 0 h (top) and 48 h (down), respectively.

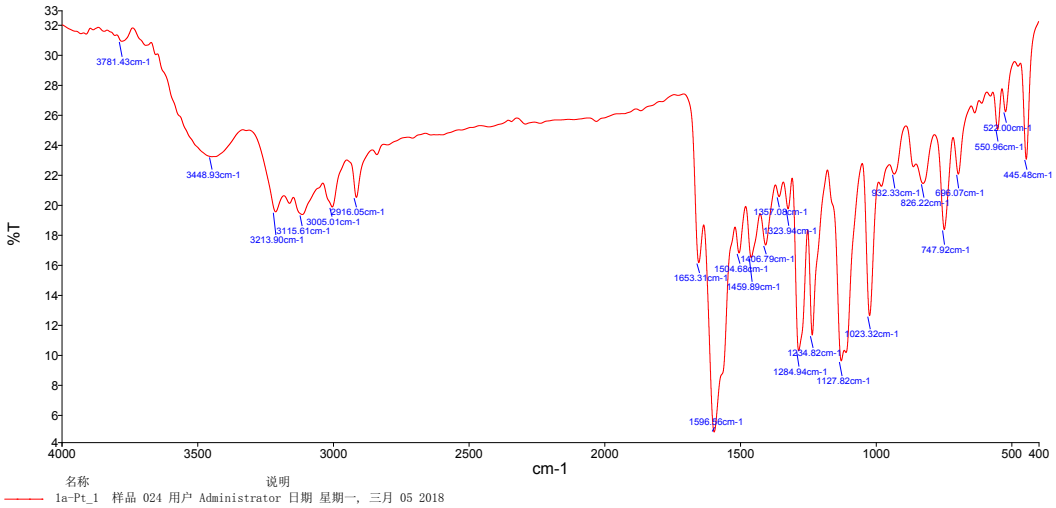

Fig. S7. IR (KBr) spectra of **Pt2**

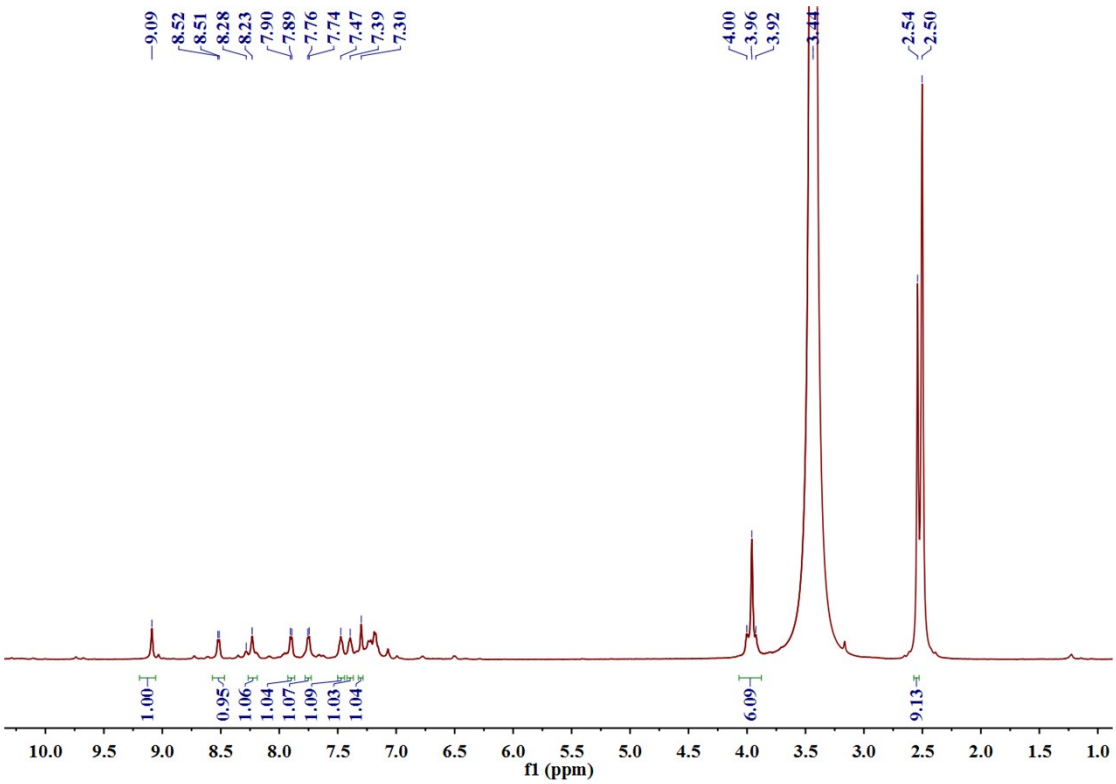

Fig. S8. ^{1}H NMR (600MHz, DMSO-d_6) for **Pt2**

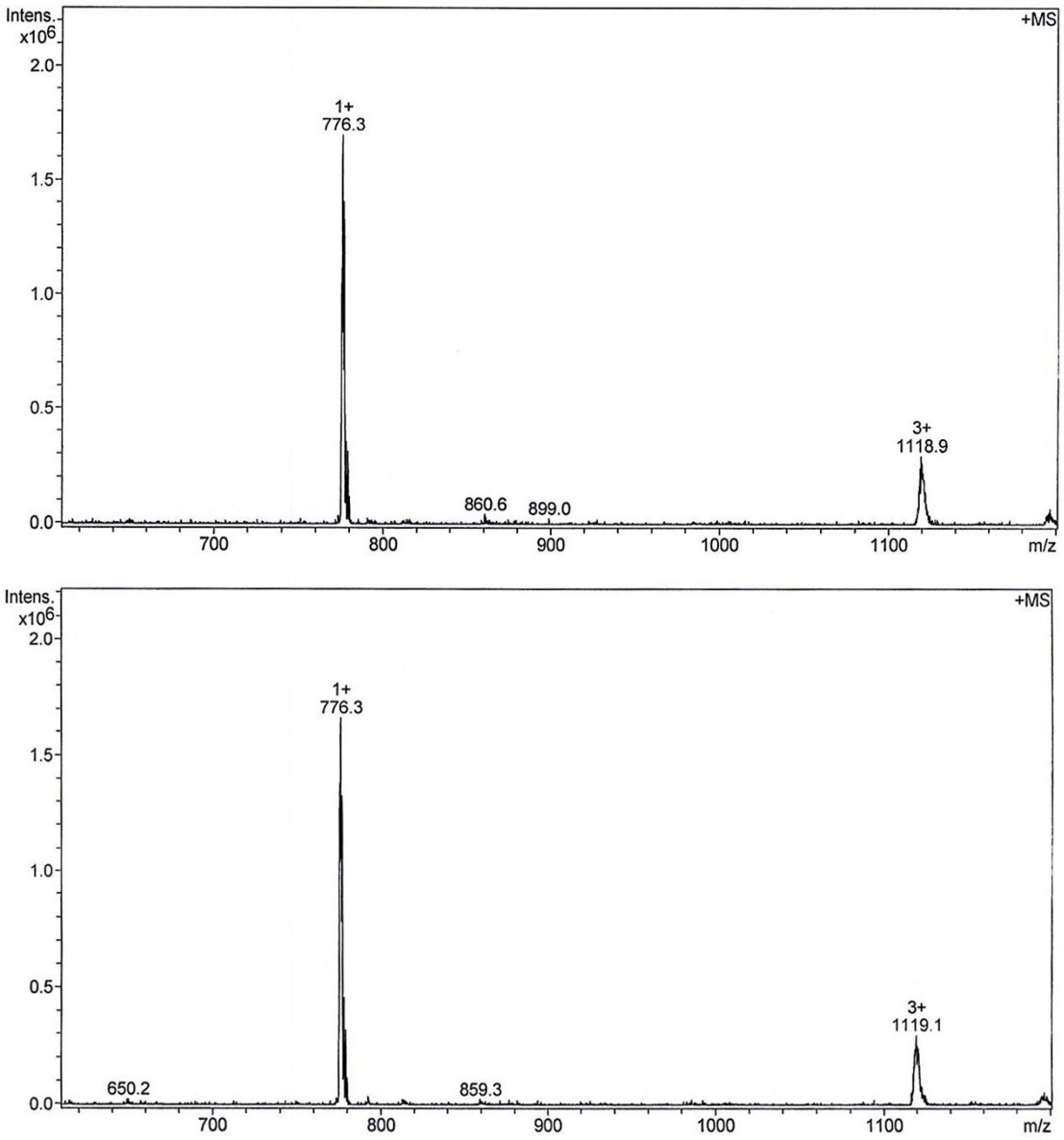

Fig. S9. The mass spectra of **Pt2** in Tris-HCl buffer solution (containing 5% DMSO) for 0 h (top) and 48 h (down), respectively.

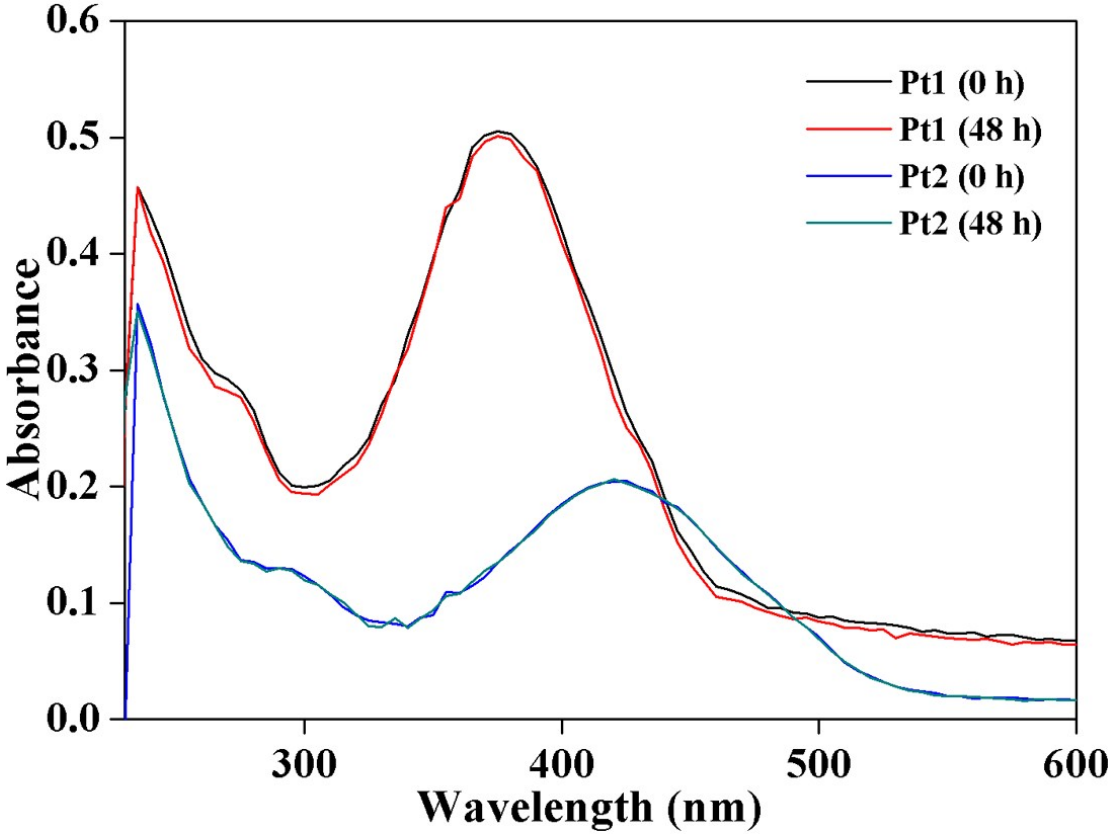

Fig. S10. UV-Vis absorption spectra of **Pt1** and **Pt2** (2.0×10^{-5} M) in TBS (Tris-HCl buffer solution, 10 mM, pH 7.35) solution in the time course 0 and 48 h, respectively.

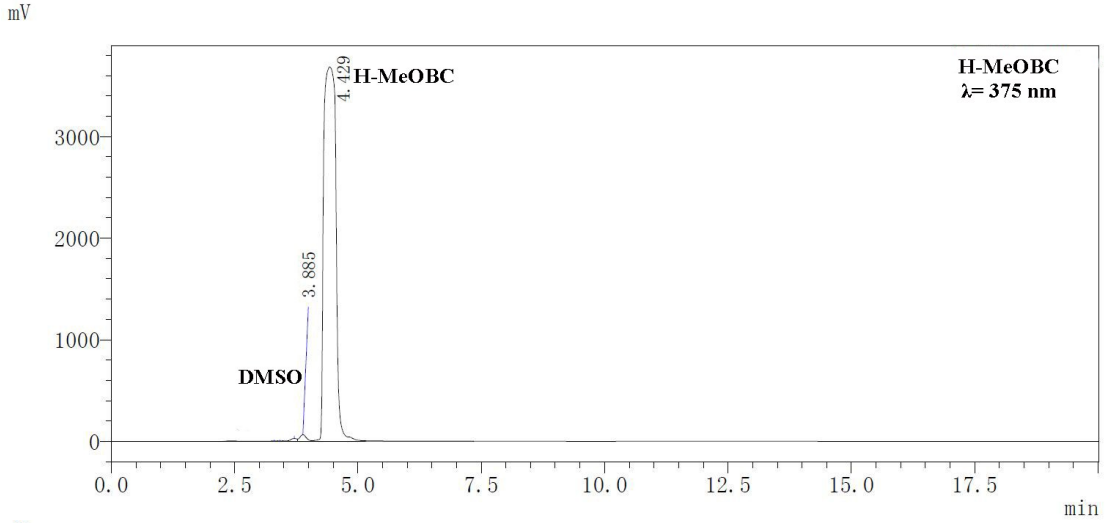
mV
H-MeOBC
λ= 375 nm
4.429
H-MeOBC
3.885
DMSO
3000
2000
1000
0
0.0
2.5
5.0
7.5
10.0
12.5
15.0
17.5
min

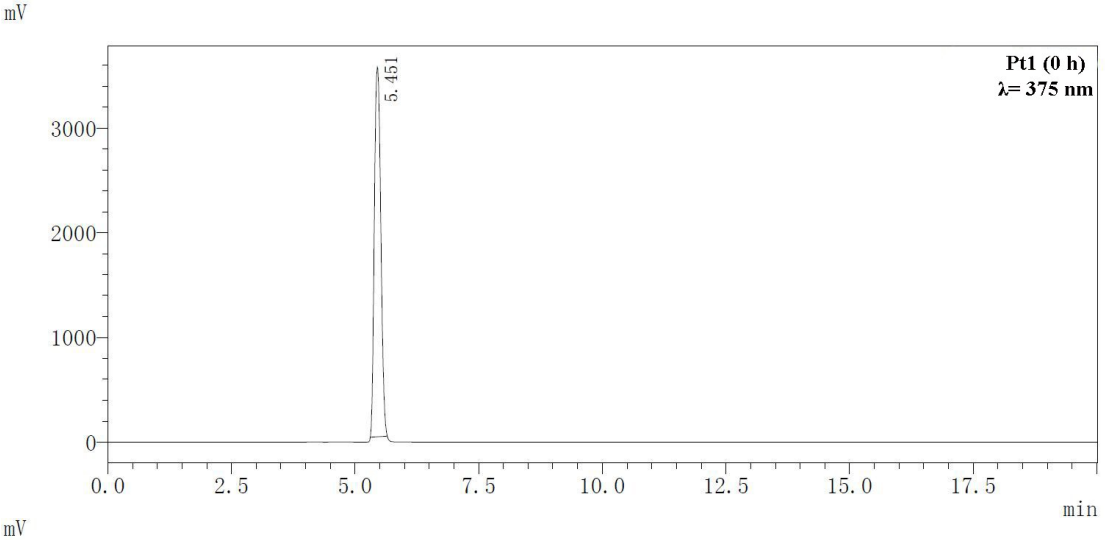
mV
Pt1 (0 h)
λ= 375 nm
5.451
3000
2000
1000
0
0.0
2.5
5.0
7.5
10.0
12.5
15.0
17.5
min

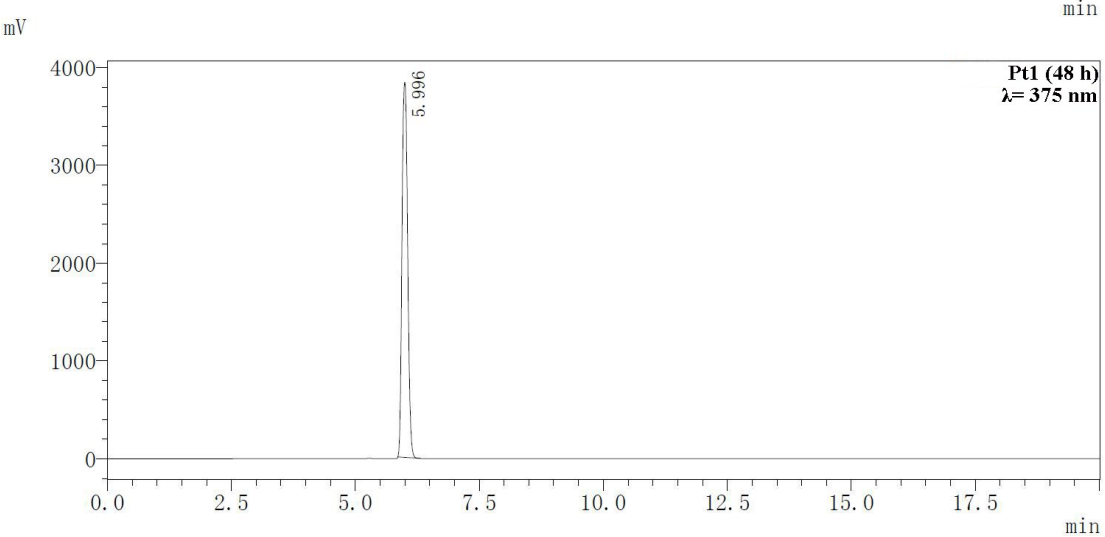
mV
Pt1 (48 h)
λ= 375 nm
5.996
4000
3000
2000
1000
0
0.0
2.5
5.0
7.5
10.0
12.5
15.0
17.5
min

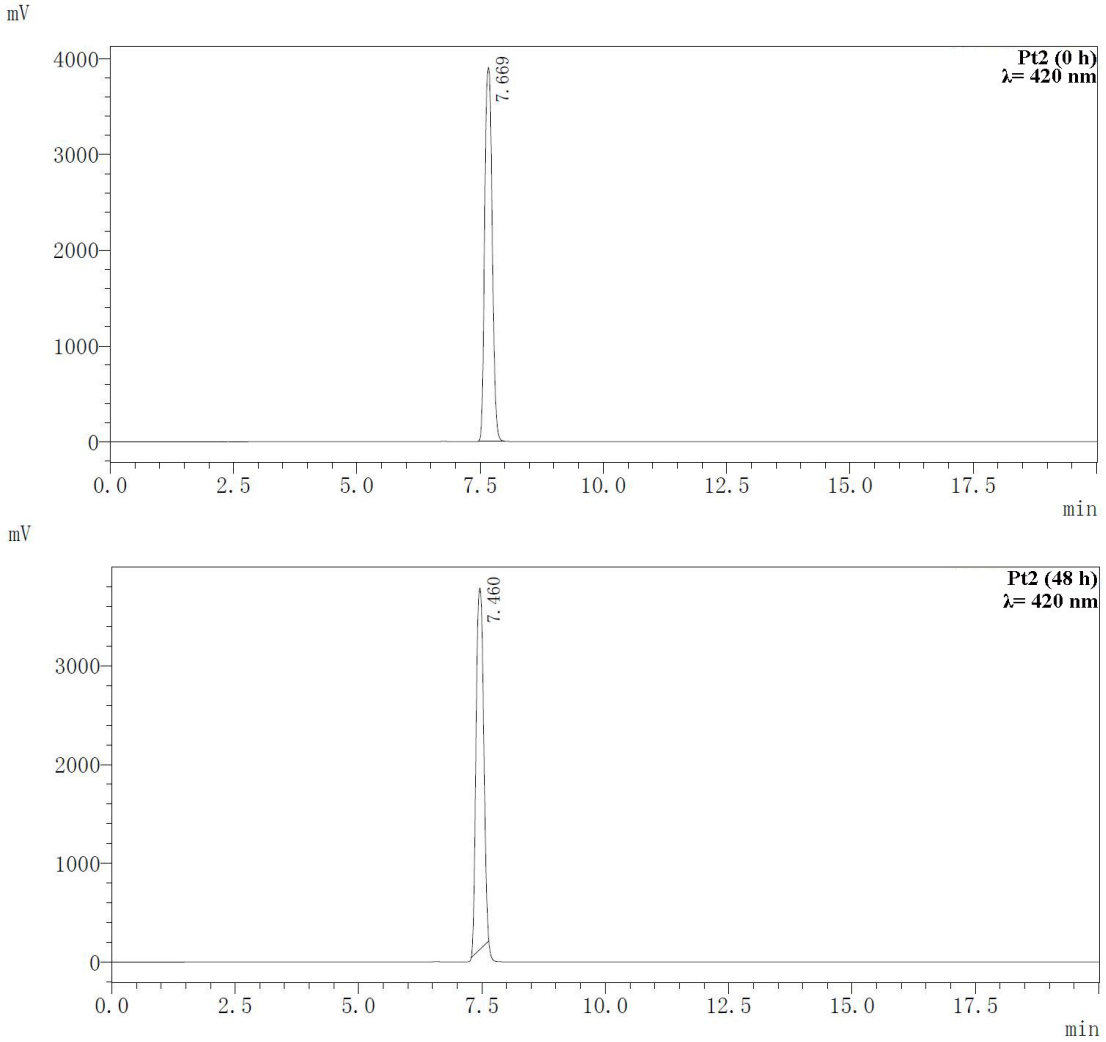

Fig. S11. HPLC spectra for the H-MeOBC ligand and its two Pt(II) complexes (2.0×10^{-3} M) in DMSO with 0 h and 48 h, respectively. Column: Inertsustain C18 column (LC-20AT, SPD-20A HPLC COLUMN, 150mm×5.0 μm I.D.). Column temperature: 40 ºC. Mobile phase: methol/H_2O containing 0.01% TFA (90:20 methol/H_2O). Flow rate: 1.0 mL/min. Injection volume: 2.0×10^{-5} M.

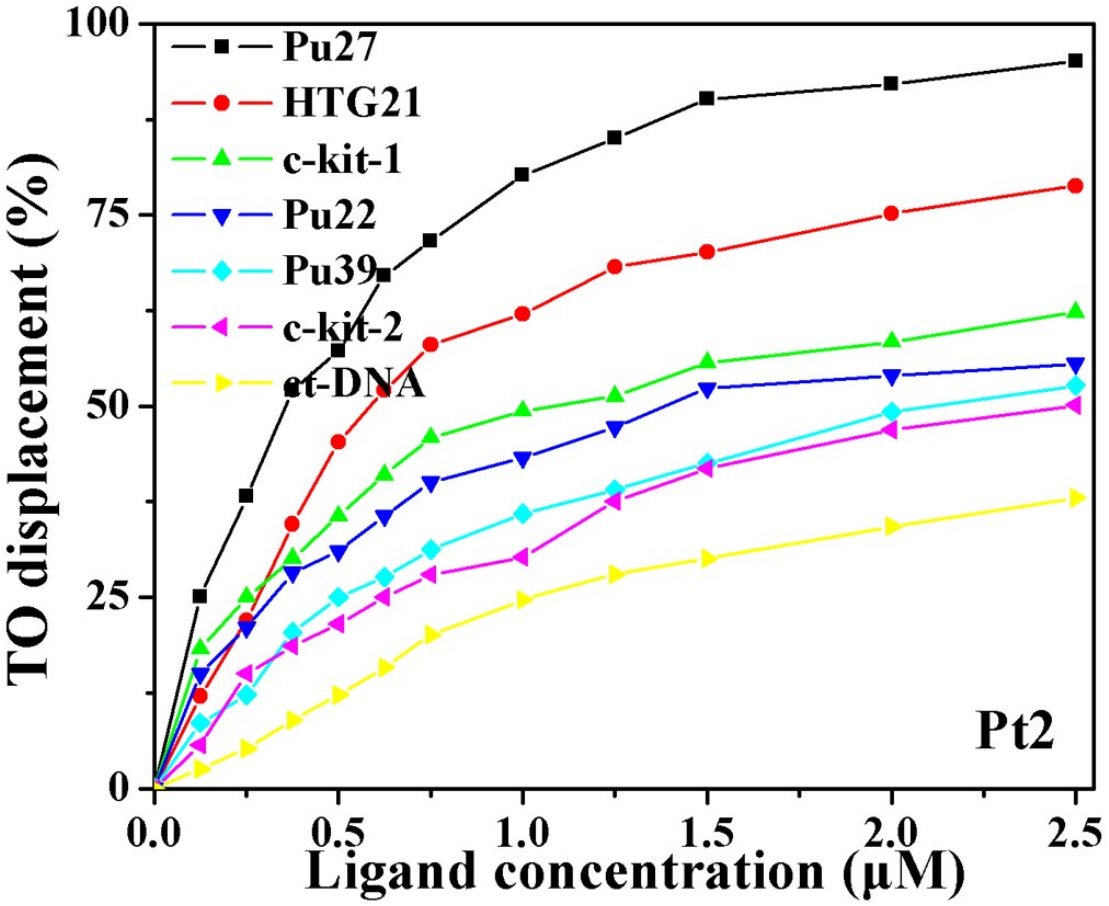

Fig. S11. FID Assay for **Pt2** on DNA

Table S8. FID assay for **Pt2** on DNA.

DC_{50}	**Pt2**
$^{Pu27}DC_{50}$	0.35
$^{HTG21}DC_{50}$	0.59
$^{c\text{-}kit\text{-}2}DC_{50}$	2.50
$^{c\text{-}kit\text{-}1}DC_{50}$	1.07
$^{Pu22}DC_{50}$	1.39
$^{Pu39}DC_{50}$	2.09
$^{ctDNA}DC_{50}$	＞2.5

DC_{50} obtained with μM.

Table S9. Sequences of oligomers (primers) used in this work, which were obtained from Shanghai Sangon Biological Engineering Technology & Services (Shanghai, China).

oligomer	sequence
Pu27	5′-TGGGGAGGGTGGGGAGGGTGGGGAAGG-3′
Pu39	5′-AGGGGCGGGCGCGGGAGGAAGGGGGCGGGAGCGGGGCTG-3′
c-kit-2	5′-CGGGCGGGCGCTAGGGAGGGT-3′
HTG21	5′-GGGTTAGGGTTAGGGTTAGGG-3′
c-kit-1	5′-CGGGCGGGCACGAGGGAGGGT-3′
Pu22	5′-TGAGGGTGGGTAGGGTGGGTAA-3′
c-myc	Ts: 5′-TGGTGCTCCATGAGGAGACA-3′
	Cx: 5′-GTGGCACCTCTTGAGGACCT-3′
hTERT	Ts: 5′-TGGTCTCCACGAGCCTCCGAGCG-3′
	Cx: 5′-CATCCACATAGAGGCCACCACGT-3′
GAPDH	Ts: 5′-GCCTCTTGCACGACCAACTG-3′
	Cx: 5′-CGGAAGGCCATGCCT GTCAG-3′

Table S10. Abbreviations in this work

TBS	Tris-HCl buffer
MTT	3-(4,5-dimethylthiazol-2-yl)-2,5-diphenyltetrazolium bromide
ROS	reactive oxygen species
IC_{50}	half maximal inhibitory concentration
G4 DNA	G-quadruplex DNA
MGC80-3 cells	human gastric mucous adenocarcinoma cells
SK-OV-3/DDP cells	human cisplatin-resistant SK-OV-3 cells
Hep-G2 cells	human hepatocellular carcinoma cells
SK-OV-3 cells	human ovarian cancer cells
HeLa cells	human sarcoma HeLa cancer cells
HL-7702 cells	human normal hepatocytes cells
PI	propidium iodide
$\Delta\psi$	mitochondrial membrane potential
JC-1	5,5′,6,6′-tetrachloro-1,1′,3,3′-tetraethylbenzimidazolylcarbocyanine

Experimental methods

Materials. Tris, RNase A, and propidium iodide (PI) were purchased from Sigma. The antibody of c-myc, hTERT, 53BP1, Cdc25 C, cyclin B, CDK2, apaf-1 and cytochrome c were purchased from Abcam. Unless otherwise stated, spectroscopic titration experiments were carried out in 10 mM Tris-HCl (pH 7.35) containing 100 mM KCl. The total RNA isolation kit and the two-step RT-PCR kit were purchased from TIANGEN. All tumor cell lines (HeLa, Hep-G2, SK-OV-3, MGC80-3, SK-OV-3/DDP tumor cells and one normal HL-7702 cells) were obtained from the Shanghai Institute for Biological Science (China). Stock solutions of the H-MeOBC ligand and its two Pt(II) complexes (2.0×10^{-3} M) were made in DMSO, and further dilutions to working concentrations were made with corresponding buffer.

Instrumentation. Infrared spectra were obtained on a Perkine Elmer FT-IR Spectrometer. Elemental analyses (C, H, N) were carried out on a Perkin Elmer Series II CHNS/O 2400 elemental analyser. NMR spectra were recorded on a Bruker AV-500 NMR spectrometer. Fluorescence measurements were performed on a Shimadzu RF-5301/PC spectro fluorophotometer. ESI-MS spectra were obtained on Thermofisher Scientific Exactive LC-MS spectrometer (ThermalElctronic, USA). The circular dichroic spectra of DNA were obtained on a JASCO J-810 automatic recording spectropolarimeter operating at 25 °C. The region between 200 and 400 nm was scanned for each sample. MTT assay was performed on M1000 microplate reader (Tecan Trading Co. Ltd, Shanghai, China). Cell cycle and apoptosis analysis was recorded on FACS Aria II Flow Cytometer (BD Biocsiences, San Jose, USA).

Cytotoxicity assay. The cell culture was maintained on RPMI-1640 medium supplemented with 10% fetal bovine serum, 100 U/mL penicillin and 100 μg/mL streptomycin in 25 cm^2 culture flasks at 37 °C humidified atmosphere with 5% CO_2.

All the cells to be tested in the following assays have a passage number of 3-6.

Cells 5.0×10^3 (HeLa, Hep-G2, SK-OV-3, MGC80-3, SK-OV-3/DDP tumor cells and one normal HL-7702 cells) per well were seeded in triplicate in 96-well plates and incubated for 24 h at 37 °C and 5% CO_2/95% air. Then graded amounts of compound were added to the wells in 10 μL of FBS free culture medium and the plates were incubated in a 5% CO_2 humidified atmosphere for 48 h. Six replica wells were used as controls. Cells were grew for 12 h before treatment to reach 70% confluency and 20 μL of tested various concentrations of compounds were added to each well. The final concentration of the tested compounds were kept at 1.25, 2.5, 5, 10, 20, 40, 50, 60, 100, 150 μM, respectively. After 48 h of culture, 0.1 mg of MTT (in 20 μL of PBS) was added to each well, and cells were incubated at 37 °C for 6 h. The formed formazan crystals were then dissolved in 100 μL of DMSO and the absorbance was read by enzyme labeling instrument with 490/630 nm double wavelength measurement. The final IC_{50} values were calculated by the Bliss method (n = 5). All tests were repeated in at least three independent trials.

Cellular uptake of Pt1 and Pt2 in SK-OV-3/DDP cells. The SK-OV-3/DDP tumor cells (~10 million cells) were treated with **Pt1** (10.0 μM), **Pt2** (0.5 μM) and cisplatin (70.0 μM) for 24 h at 37 °C in a humidified 5% CO_2 incubator. The spent media was removed, and the cells were washed with 5 mL of PBS, scraped, and collected in 5 mL of PBS. The scrapped cells were spun down, by centrifuging at 2500 rpm for 10 min. The cell pellet obtained was dissolved in 1 M NaOH (1 mL) and diluted with 2% (v/v) HNO_3 (5 mL) for determining whole cell cobalt content. Another set was treated similarly, nuclear fraction, nuclear proteins, membrane proteins and cytoplasmic protein were isolated as described by Schreiber et al [1], and the final solution was made up to 5 mL using 2% (v/v) HNO_3. The amount of cobalt

taken up by the cells was determined by ICP-MS. The instrument was calibrated for Pt complexes using standard solutions containing 10, 50, 100, 500 and 1000 ppb Pt.

Cell apoptosis analysis. Apoptosis was detected by flow cytometric analysis of annexin V staining. Annexin V-FITC vs PI assay was performed as previously described [1-3]. Briefly, adherent SK-OV-3/DDP cancer cells were harvested and suspended in the annexin-binding buffer (5×10^5 cells/mL). Then, the SK-OV-3/DDP cancer cells after treated with **Pt1** (10.0 μM), cisplatin (70.0 μM) and **Pt2** (0.5 μM) were incubated with annexin V-FITC and PI for 1 h at room temperature in the dark and immediately analyzed by flow cytometry. The data are presented as biparametric dot plots showing PI red fluorescence vs annexin V-FITC green fluorescence.

Cell cycle analysis. In cell cycle analysis, the SK-OV-3/DDP cancer cells were maintained with 10% fetal calf serum in 5% CO_2 at 37 °C. The cells after after treated with **Pt1** (10.0 μM) and **Pt2** (0.5 μM) were harvested by trypsinization and rinsed with PBS. After centrifugation, the pellet (10^5–10^6 cells) was suspended in 1 mL PBS. The cells were washed in PBS and fixed with ice-cold 70% ethanol in PBS under violent shaking. Cells 1×10^6 were centrifuged and resuspended in a staining solution (0.5 mL of PBS containing 50 μg/mL PI and 75 kU/mL RNase A) for 30 min at room temperature in the dark. Finally, the cell cycle was analyzed by FACS Calibur flow cytometer (BD) and the cell cycle distribution and percentage of apoptotic cells were analyzed using Cell Quest (BDIS) and ModFit LT (Verity Software House, Topsham, ME).

Induction of ROS in SK-OV-3/DDP cells. DCFH-DA is a freely permeable tracer specific for ROS. At the same time, DCFH-DA can be deacetylated by intracellular esterase to the non-fluorescent DCFH which is oxidized by ROS to the fluorescent compound 2',7'-dichloroflorescein (DCF). Therefore, the fluorescence intensity of

DCF is proportional to the amount of ROS produced by the cells [4-6]. T-24 cells 1×10^6 were exposed to **Pt1** (10.0 μM) and **Pt2** (0.5 μM) for 24 h, respectively, and 1 mM H_2O_2 used as a positive control of ROS production. After the exposure, cells were harvested, washed once with ice-cold PBS and incubated with DCFH-DA (100 μM in a final concentration) at 37 ºC for 15 min in the dark [5,6]. Finally, the cells were washed again and maintained in 1 mL PBS. The ROS generation was assessed from 10,000 cells each sample by flow cytometric analysis with excitation and emission wavelengths of 488 and 530 nm, respectively.

Δψm loss. The loss of mitochondrial membrane potential (Δψ) was assessed using a lipophilic cationic fluorescent probe, JC-1 (5,5′,6,6′-tetrachloro-1,1′,3,3′-tetraethylbenzimidazolylcarbocyanine; Beyotime). SK-OV-3/DDP tumor cells treated with **Pt1** (10.0 μM) and **Pt2** (0.5 μM) for 24 h were incubated with 5 μg/mL JC-1 for 30 min at 37 °C and examined under the fluorescence microscopy. The emission fluorescence for JC-1 was monitored at 530 and 590 nm, under the excitation wavelength at 488 nm. These cells were treated with **Pt1** (10.0 μM) and **Pt2** (0.5 μM) for 24 h and then analyzed by JC-1 flow cytometry.

Induction of Ca^{2+} fluctuation in SK-OV-3/DDP cells. The level of intracellular free Ca^{2+} is decided by using a fluorescent dye Fluo-3 AM which can across the cell membrane and be cut into Fluo-3 by intracellular esterase. The Fluo-3 can specifically combine with the Ca^{2+} and has a strong fluorescence with an excitation wavelength of 488 nm. After exposed to **Pt1** (10.0 μM) and **Pt2** (0.5 μM) for 24 h, respectively, the SK-OV-3/DDP tumor cells were harvested and washed twice with PBS, then resuspended in Fluo-3 AM (5.0 mM) for 30 min in dark. Detection of intracellular Ca^{2+} was carried by Flow cytometer at 525 nm excitation wavelength.

Telomerase activity. The telomerase extract was prepared from the SK-OV-3/DDP

cance cells: a total of 5 × 10^6 SK-OV-3/DDP tumour cells untreated or treated with **Pt1** (10.0 μM) and **Pt2** (0.5 μM) were pelleted, and the cells were washed with 5 mL of PBS, scraped and lysed for 30 min on ice. Finally, the lysate was centrifuged at 13000 rpm for 30 min at 4 °C; the supernatant was collected and stored at −80 °C before use [6,7]. The TRAP assay was performed by following previously published procedures [7-9]. Telomerase extract was prepared from SK-OV-3/DDP cancer cells. A modified version of the TRAP assay was used [8]. PCR was performed in a final 50 mL reaction volume composed of reaction mix (45.0 mL) containing Tris-HCl (20 mM, pH 8.0), deoxynucleotide triphosphates (50 mM), $MgCl_2$ (1.5 mM), KCl (63 mM), EGTA (1 mM), Tween-20 (0.005%), BSA (20 mg/mL), primer H21T (3.5 pmol; 5'-$G_3[T_2AG_3]_3$-3'), primer TS (18 pmol; 5'-AATCCGTCGAGCAGAGTT-3'), primer Cxext (22.5 pmol; 5'-GTGCCCTTACCCTTACCCTTACCCTAA-3'), primer NT (7.5 pmol; 5'-ATCGCTTCTCGGCCTTTT-3'), TSNT internal control (0.01 amol; 5'-ATTCCGTCGAGCAGAGTTAAAAGGCCGAGAAGCGAT-3'), Taq DNA polymerase (2.5 U), and telomerase (100 ng). Compounds or distilled water was added (5 mL). PCR was performed in an Eppendorf Master cycler equipped with a hot lid and incubated for 30 min at 30 °C, followed by 92 °C 30 s, 52 °C 30 s, and 72 °C 30 s for 30 cycles. After amplification, loading buffer (8 mL; 5×TBE buffer, 0.2% bromophenol blue, and 0.2% xylene cyanol) was added to the reaction. An aliquot (15 mL) was loaded onto a nondenaturing acrylamide gel (16%; 19:1) in 1×TBE buffer and resolved at 200 V for 1.5 h. Gels were fixed and then stained with $AgNO_3$.

RNA extraction. SK-OV-3/DDP tumour cells pellets harvested from each well of the culture plates were lysed in RZ Lysis solution. RNA was extracted with RNAsimple Total RNA kit (TIANGEN) according to manufacturer's protocol and eluted in distilled, deionized water with 0.1% diethyl pyrocarbonate (DEPC) to a final

volume of 50 μL. RNA was stored at −150 °C before use.

RT-PCR assay. Total RNA was used as a template for reverse transcription using the following protocol: each 20 μL reaction contained 2.0 μL 10×RT mix., 2.0 μL dNTP (2.5 mM), 2.0 μL Oligo-dT15 primer, 1.0 μL Quant Reverse Transcriptase, 10 μL DEPC-H_2O, and 2 μg of total RNA. Briefly, RNA and oligo dT15 primer was incubated at 37 °C for 60 min and then immediately placed on ice. Finally, the reacted solution was stored at −80℃. Real-time PCR was performed on 7500fast Real-Time PCR (ABI Co. Ltd, USA) by using 2.5×RealMasterMix/20×SYBR solution (TIANGEN), according to the manufacturer's protocol. The total volume of 20.0 μL real-time RT-PCR reaction mixtures contained 9.0 μL of 2.5×RealMasterMix/20×SYBR solution, 0.25 μM each of forward and reverse primers, 1.0 μL of cDNA, and nuclease-free water. The program used for all genes consisted of a denaturing cycle of 3 min at 95 °C, 45 cycles of PCR (95 °C for 20 s, 58 °C for 30 s, and 68 °C for 30 s), a melting cycle consisting of 95 °C for 15 s, 65 °C for 15 s, and a step cycle starting at 65 °C with a 0.2 °C/s transition rate to 95 °C. The specificity of the real-time RT-PCR product was confirmed by melting curve analysis. The PCR product sizes were confirmed by agarose gel electrophoresis and ethidium bromide staining. Three replications were performed, and then hTERT and c-myc mRNA levels were normalized with the GAPDH mRNA level of each sample. Results of real-time PCR were analyzed using the $2^{-\Delta\Delta CT}$ method in the program Origin 8.0 to compare the transcriptional levels of hTERT and c-myc genes in each sample relative to nondrug treated control.

Western blotting. The SK-OV-3/DDP tumor cells after treated with **Pt1** (10.0 μM), **Pt2** (0.5 μM) and cisplatin (70.0 μM) harvested from each well of the culture plates were lysed in 150 μL of extraction buffer consisting of 149 μL of RIPA Lysis

Buffer and 1 μL PMSF (100 mM). The suspension was centrifuged at 10000 rpm at 4 °C for 10 min, and the supernatant (10 μL for each sample) was loaded onto 10% polyacrylamide gel and then transferred to a microporous polyvinylidene difluoride (PVDF) membrane. Western blotting was performed using anti- c-myc, hTERT, 53BP1, Cdc25 C, cyclin B, CDK2, apaf-1, cytochrome c and β-actin antibody and horseradish peroxidase-conjugated antimouse or antirabbit secondary antibody. Protein bands were visualized using chemiluminescence substrate.

Transfection assay. After the SK-OV-3/DDP tumor cells (1.0×10^6) were grew in 3 cm Petri dishes for 24 h, DNA transfections were performed using the following procedure. Firstly, 2.0 μg EGFP plasmid [10] and 2.0 μg c-myc plasmid [11,12] were cotranfected into T-24 cancer cells using Lipo2000 (Invitrogen). Then, **Pt1** (10.0 μM) and **Pt2** (0.5 μM) were added into medium, respectively, after 6.0 h of transfection. After another 24 h of drug treatment, the cells were imaged using Nikon TE2000 (Japan) scanning fluorescence microscope and studied by Luciferase Reporter Gene Assay Kit.

Statistical analysis. The experiments have been repeated from three to five times, and the results obtained were presented as means±standard deviation (SD). Significant changes were assessed by using Student's *t* test for unpaired data, and p values of <0.05 were considered statistically significant.

References

1 E. Schreiber, P. Matthias, M. M. Mueller and W. Schaffner, Rapid detection of octamer binding proteins with'mini-extracts', prepared from a small number of cells, Nucleic Acids Res., 1989, **17**, 6419.

2 L. Chong, B. van Steensel, D. Broccoli, H. Erdjument-Bromage, J. Hanish, P. Tempst and T. de Lange, A human telomeric protein, Science, 1995, **270**, 1663–1667.

3 D. Broccoli, A. Smogorzewska, L. Chong and T. de Lange, Human telomeres contain two distinct Myb–related proteins, TRF1 and TRF2, Nat. Genet., 1997, **17**, 231–235.

4 S. Lin, M. Fujii and D. X. Hou, Rhein induces apoptosis in HL-60 cells via reactive oxygen species-independent mitochondrial death pathway, Arch. Biochem. Biophys., 2003, **418**, 99–107.

5 R. M. Sainz, J. C. Mayo, D. X. Tan, S. Lopez-Burillo, M. Natarajan and R. J. Reiter, Antioxidant activity of melatonin in Chinese hamster ovarian cells: changes in cellular proliferation and differentiation, Biochem. Bioph. Res. Commun., 2003, **302**, 625–634.

6 Z.-F. Chen, Q.-P. Qin, J.-L. Qin, Y.-C. Liu, K.-B. Huang, Y.-L. Li, T. Meng, G.-H. Zhang, Y. Peng, X;-J. Luo and H. Liang, Stabilization of G-quadruplex DNA, inhibition of telomerase activity, and tumor cell apoptosis by organoplatinum(II) complexes with oxoisoaporphine, J. Med. Chem., 2015, **58**, 2159–2179.

7 A. De Cian, G. Cristofari, P. Reichenbach, E. De Lemos, D. Monchaud, M.-P. Teulade-Fichou, K. Shin-ya, L. Lacroix, J. Lingner and J.-L. Mergny,

Reevaluation of telomerase inhibition by quadruplex ligands and their mechanisms of action, PNAS, 2007, **104**, 17347–17352.

8 J. E. Reed, A. A. Arnal, S. Neidle, R. Vilar, Stabilization of G-quadruplex DNA and inhibition of telomerase activity by square-planar nickel(II) complexes, J. Am. Chem. Soc., 2006, **128**, 5592–5993.

9 G. Krupp, K. Kühne, S. Tamm, W. Klapper, K. Heidorn, A. Rott and R. Parwaresch, Molecular basis of artifacts in the detection of telomerase activity and a modified primer for a more robust 'TRAP'assay, Nucleic Acids Res., 1997, **25**, 919–921.

10 M. Chalfie, Y. Tu, G. Euskirchen, W. W. Ward and D. C. Prasher, Green fluorescent protein as a marker for gene expression, Science, 1994, **263**, 802–805.

11 T.-C. He, A. B. Sparks, C. Rago, H. Hermeking, L. Zawel, L. T. da Costa, P. J. Morin, B. Vogelstein and K. W. Kinzler, Identification of c-MYC as a target of the APC pathway, Science, 1998, **281**, 1509–1512.

12 Q.-P. Qin, T. Meng, M.-X. Tan, Y.-C. Liu, X.-J. Luo, B.-Q. Zou and H. Liang, Synthesis and in vitro biological evaluation of three 4′-(4-methoxyphenyl)-2,2′:6′,2″-terpyridine iridium(III) complexes as new telomerase inhibitors, Eur. J. Med. Chem., 2018, **143**, 1387–1395.

13 T. Meng, S.-F. Tang, Q.-P. Qin, Y.-L. Liang, C.-X. Wu , C.-Y. Wang, H.-T. Yan, J.-X. Dong and Y.-C. Liu, Evaluation of the effect of iodine substitution of 8-hydroxyquinoline on its platinum(II) complex: Cytotoxicity, cell apoptosis and telomerase inhibition, Med. Chem. Commun., 2016, **7**, 1802–1811.